

1076 (1974); M. Yamada, H. W. Hendel, S. Seiler, and S. Ichimaru, *Phys. Rev. Lett.* **34**, 650 (1975); P. D. Edgley, R. N. Franklin, S. M. Hamberger, and R. W. Motley, *Phys. Rev. Lett.* **34**, 1269 (1975).

²N. Rynn, D. R. Dakin, D. L. Correll, and Gregory Benford, *Phys. Rev. Lett.* **33**, 765 (1974); D. L. Correll, N. Rynn, and H. Böhmer, *Phys. Fluids* **18**, 1800 (1975); D. R. Dakin, T. Tajima, G. Benford, and N. Rynn, *J. Plasma Phys.* **15**, 175 (1976).

³N. S. Buchelnikova and R. A. Salimov, *Zh. Eksp. Teor. Fiz.* **56**, 1108 (1969) [*Sov. Phys. JETP* **29**, 595 (1969)].

⁴J. M. Kindel and C. F. Kennel, *J. Geophys. Res.* **76**, 3055 (1971); M. C. Kelley, E. A. Bering, and F. S. Mozer, *Phys. Fluids* **18**, 1590 (1975).

⁵See, for example, F. H. Coensgen, W. F. Cummins, B. G. Logan, A. W. Molvik, W. E. Nexsen, T. C. Simonen, B. W. Sallard, and W. C. Turner, *Phys. Rev. Lett.* **35**, 1501 (1975).

⁶R. A. Stern and J. A. Johnson, III, *Phys. Rev. Lett.* **34**, 1548 (1975); C. F. Burrell and H. J. Kunze, *Phys. Rev. Lett.* **28**, 1 (1975), and **29**, 1445 (1975); and D. Dimock, E. Hinnov, and L. C. Johnson, *Phys. Fluids* **12**,

1730 (1969).

⁷W. Gekelman, T. R. Hart, K. C. Rogers, and R. O. Motz, *Appl. Phys. Lett.* **21**, 510 (1972).

⁸R. A. Stern, D. L. Correll, H. Böhmer, and N. Rynn, University of California at Irvine Report No. 76-36 (unpublished). Our technique, based on the proper use of intensity rules and low-power cw laser beams, yields higher signals and reduces Zeeman-Doppler interference.

⁹The laser linewidth $\leq 0.03 \text{ \AA}$ is broader for all but the last point ($T_i \leq 2.4 \times 10^4 \text{ K}$) in Fig. 3, curves *a* and *b*, rendering intensity corrections for Doppler broadening unnecessary. For the last point, less than 30% of the ions lie outside the laser linewidth. This correction brings the density closer to the dashed line.

¹⁰W. E. Drummond and M. N. Rosenbluth, *Phys. Fluids* **5**, 1507 (1962).

¹¹The increased fluorescence intensity 5 mm outside the filament cannot be due to electron heating, which would require 10^9 K for Larmor radii extending so far out.

¹²R. N. Motley and N. D'Angelo, *Phys. Fluids* **6**, 296 (1963).

Preheat by Fast Electrons in Laser-Fusion Experiments

B. Yaakobi, I. Pelah,* and J. Hoose

Laboratory for Laser Energetics, University of Rochester, Rochester, New York 14627

(Received 24 March 1976)

Neon-filled glass spherical shell targets were irradiated by a four-beam laser system of incident power 0.6–0.8 TW. By measuring $K\alpha$ x-ray lines of neon and silicon we are able to determine the number of fast (nonthermal) electrons and their preheating effect. Correlation is made with fast ion measurements.

Premature heating of the interior of laser-irradiated targets by either fast electrons or x rays has long been recognized as one of the most serious difficulties to contend with in fusion experiments.¹ For example, preheat of the gas enclosed in glass spherical shells should make it more difficult to compress it; preheat of the inner part of the glass shell would cause it to explode inwards and the "pusher" action is thereby impaired. We have studied preheat *experimentally* by measuring the intensity of $K\alpha$ radiation from the glass elements as well as from a heavy fill gas, neon. Electrons or x rays of sufficient energy traveling into cold un-ionized material can eject K -shell electrons before the outer electrons are removed through heating. A K -shell vacancy has a probability ω (the fluorescence yield) to decay by emitting a $K\alpha$ photon. The fraction $1-\omega$ of the absorbed energy is mostly converted into heat, either through Auger cascades or through the emission of softer radiation which

has a high probability of being reabsorbed. If preheat continues as the target core is being heated and ionized through compression, $K\alpha$ lines will shift to shorter wavelengths one step for each additional removed electron.²

The targets used in this study were glass spherical shells of diameter about 90 μm and wall thickness 1 μm filled with neon of pressures 2 and 10 atm. $K\alpha$ lines of neon can be excited by electrons of energies higher than 0.87 keV. A heavier atom fill gas (e.g., argon) would detect electrons above a higher threshold. Since fast electrons are believed to be produced near the critical surface these results should apply to other gas fills, such as D - D or D - T . Other experimental parameters were total incident power in four beams 0.6–0.8 TW, power density $(2-3) \times 10^{15} \text{ W/cm}^2$, pulse width 0.2–0.4 nsec, and energy absorbed 5–10 J. For more details on the laser system and interaction diagnostics see Soures, Goldman, and Lubin.³ A saturable dye

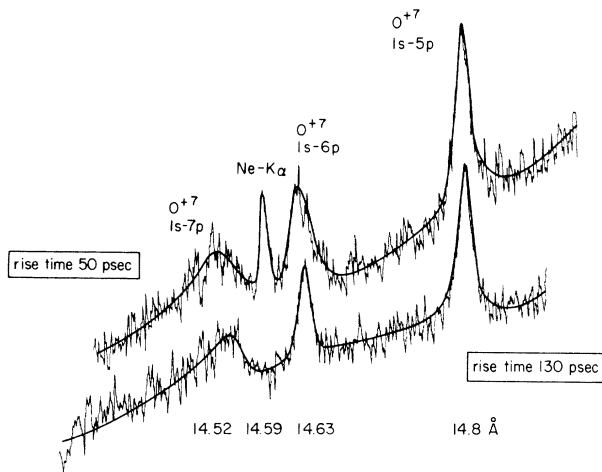


FIG. 1. X-ray oxygen lines from laser-irradiated glass microballoons and the $K\alpha$ line from the neon fill gas. The main difference between the two experiments is in the laser pulse rise time, but it is not clear whether this was the reason for the difference in the spectrum.

cell was inserted in the laser path in some of the experiments and was found to affect the results.

The experimental results are summarized in Figs. 1 and 2. $K\alpha$ radiation of silicon appeared when the dye cell was inserted in the laser path. $K\alpha$ radiation of neon appeared when the dye cell was used and the neon pressure was 10 atm. Consequently, the analysis below refers to this fill pressure only. Two lines in Figs. 2(a) and 2(b) are tentatively identified as $K\alpha$ transitions in neon where one outer electron has been removed. The longer wavelength agrees within experimental error with the calculated² wavelength 14.518 \AA for the transition $1s2s^22p^5-1s^22s^22p^4$. The identification of the shorter wavelength ($\sim 14.47 \text{ \AA}$) is uncertain; it could be due to the transition $1s2s2p^6-1s^22s2p^5$ which has not been calculated. These two lines always appeared together, with or without the ordinary $K\alpha$ line. Presumably these differences are due to the different time histories of electron production. Using the published crystal reflection data and film calibration,⁴ we derive, for the Ne- $K\alpha$ line of Fig. 1, a total intensity of about 0.2 mJ.

In analyzing these results we assume that when $K\alpha$ radiation is emitted from essentially cold material, the target compression has not yet progressed appreciably. Supportive evidence is the fact that the density scale length near the critical layer was found to be small early in the pulse and then to grow.⁵ The laser intensity arriving at the critical layer may be therefore relatively higher

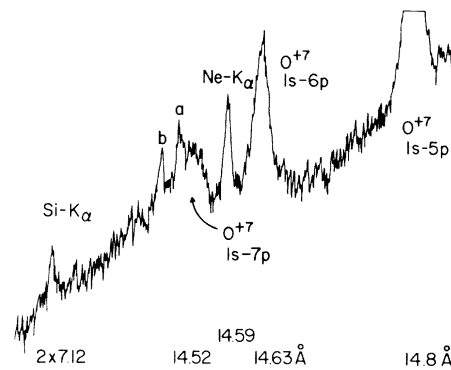


FIG. 2. A case where $K\alpha$ radiation from ionized neon as well as from neutral neon has appeared (see text). Also seen is the $K\alpha$ line of silicon in second order; heliumlike and hydrogenlike second-order lines of silicon appear to the left of the wavelength range of the figure. The background is instrumental.

early in the pulse, producing more fast electrons. Also, the fact that we have observed $K\alpha$ lines from only neutral and singly ionized species may indicate the existence of fast electrons only early, before significant compression heating takes place. We first consider the possibility that the Ne- $K\alpha$ line was excited by x rays of energy higher than the K edge (0.8 keV). We have recorded on film the spectrum in the range 0.7–3 keV. It consists of sharp and intense lines arising above a weak continuum. Most of the line intensity is from Si^{+12} and Si^{+13} ions. The continuum is due to free-free and free-bound emissions as well as fluorescence inside the spectrometer. The total integrated intensity of lines and continuum (assuming fluorescence to be negligible) was found to be about 120 times higher than that of the Ne- $K\alpha$ line. Using this lower bound on the relative intensity of the Ne- $K\alpha$ line we show it to be too intense to have been predominantly excited by x rays. The number of Ne- $K\alpha$ photons per each emitted photon from the glass shell can be estimated as $R = \omega\sigma_p n(2D/\pi)/2$. The fluorescence yield ω in neon⁶ is 0.018, σ_p is the photo-ionization cross section,⁷ n is the density of neon atoms, taken as the initial density, $(2D/\pi)$ is the average chord length in a circle of diameter D , and the factor of 2 accounts for the fact that only half of the photons travel inwards. We obtain $R = 10^{-3}$, as compared with the observed ratio which is $\approx 10^{-2}$.

Fast electrons produced near the critical layer should be confined to the pellet by the restoring positive charge; they would thus move back and forth through the pellet until stopped by energy

losses. The total Ne- $K\alpha$ line intensity due to electrons is given by

$$I(K\alpha) = \omega N(\text{neon}) N_e^f \sigma_e m h \nu / A. \quad (1)$$

Here $N(\text{neon})$ is the total number of neon atoms, 1.2×10^{14} and N_e^f is the total number of fast electrons created over the whole pulse length. It is important to realize that fast electrons in the present context can be either superthermal electrons or thermal electrons from hot spots. σ_e is the cross section⁸ for electron production of a K -shell vacancy; it changes by less than a factor of 1.5 around 10^{-20} cm^2 in the energy range 1.5–15 keV, m is the number of times an electron traverses the target before being absorbed, and A the cross-sectional area of the target taken to have its initial value. In order for this calculated intensity to equal the measured value 0.2 mJ, $m N_e^f$ has to be about 4×10^{15} . Using a simple model to describe the electrostatic interactions in the target, we show now that this value of $m N_e^f$ is in fact consistent with our fast ion measurements.

Traces of charged particle collectors corresponding to Figs. 1 and 2 show a pulse of ions of velocity $\geq 10^8 \text{ cm/sec}$ ahead of the thermally expanding pellet plasma. The total energy carried by fast ions is about 0.5 J. We assume that these ions have been accelerated by fast electrons trying to escape the target. Thus, the energy in fast electrons is being used partly to accelerate ions, partly to preheat the cold target. We conclude that fast electrons in these experiments had an energy 1 J or higher. The measured velocity of fast ions shows the potential drop across the charge-separation field to be about 10 keV (most ions should have a mass to charge ratio of about 2). The energy of electrons creating this potential drop is then also $\sim 10 \text{ keV}$ which yields for the minimum total number of fast electrons 10^{15} . We assume further that only half of the glass-shell thickness is effective in stopping the electrons, the rest has been ionized and ablated. Using range data⁹ for 10-keV electrons, we find the number of electron traversals before absorption to be $m = 5$ yielding $m N_e^f \sim 5 \times 10^{15}$, as compared with the value 4×10^{15} derived from the Ne- $K\alpha$ line intensity. From these numbers an average fast electron density $\sim 10^{19} \text{ cm}^{-3}$ can be easily derived.

The potential drop accelerating the ions equals the product of an electric field E and a separation distance d between opposite charges. The observed total charge of fast ions ($3 \times 10^{14} e$) is

larger than the total charge Q of ions within this field at any one moment by the ratio $\alpha = l/(d/v_i)$; here Δt is the duration of fast electron production and d/v_i is the time for an ion to traverse the field. The resulting charge per unit area creating the field is $q = Q/4\pi R^2$ where R is approximately the initial radius of the target and q is related to the field through the elementary equation $E = q/\epsilon_0$ or $V = Ed = qd/\epsilon_0$. We finally get $d^2 = 4\pi R^2 E_0 V v_i \Delta t / 3 \times 10^{14} e$ from which it follows that $d \sim 10^{-5} \text{ cm}$ and $E \sim 10^9 \text{ V/cm}$. We can check the consistency of these estimates as follows: Using the electron density $Q/4\pi R^2 d$ and assuming $T = 1 \text{ keV}$ we find that the Debye length at the sheath location equals $\sim d/3$, roughly as expected.

The predicted intensity ratio R of the $K\alpha$ lines of silicon to that of neon can be found from Eq. (1). The ratio of the ω values⁶ is 2.6, of N about 3, of σ_e ⁸ ~ 0.22 and of $h\nu$ ~ 2.2 , hence $R = 3.7$. The measured value in Fig. 2 can be roughly estimated^{4,10} to be $R \sim 2$.

Nonthermal electrons lose their energy either through preheat or through acceleration of ions. Preheat calculations are underway using a hydrodynamic numerical code which treats the transport of nonthermal electrons through the pellet. The total number of fast electrons measured here serves as normalization for such calculations. As an illustration let us consider the preheating effect of the fast electrons measured here (10^{15} electrons of energy 10 keV) on a 10-atm deuterium fill gas in otherwise identical conditions to those in our experiment. Under these conditions a fast electron traversing the target gives rise to about five ionization events.⁹ Since the number of fast electrons is larger than the number of deuterium atoms (2×10^{14}) it turns out that only a fraction of the fast electron energy is required to totally ionize the fill gas. The resulting electron temperature is about 20 eV (the fast electron loses 36 eV per ionization⁹ from which the ionization energy has to be subtracted). From now on the fast electrons only lose energy by Coulomb collisions which are far less efficient (about 4 eV/cm loss rate along the fast electron path).

X-ray pinhole camera images showed a ring and a strong, resolution limited central spike indicating a volume compression of at least 100. More refined methods for measuring compression would be required to see the effect of preheat on compressions in these experiments. However, as Fig. 1 indicates, oxygen lines are broader in the case when Ne- $K\alpha$ line does appear.

These lines are Stark-broadened¹¹ and show a density (of order 10^{21} cm^{-3}) which is about twice as high as when the Ne- $K\alpha$ line is absent. It seems that energy carried inwards by fast particles (mainly ions) effectively enhances the heat conduction which was found¹¹ to otherwise to be inhibited. This effect should be favorable for compression, in contrast to preheating.

This work was supported by the Laser Fusion Feasibility Project at the University of Rochester.

*Permanent address: Soreq Nuclear Research Center, Yavne, Israel.

¹G. S. Fraley and R. J. Mason, Phys. Rev. Lett. **35**, 520 (1975).

²L. L. House, Astrophys. J., Suppl. **181**, 21 (1969).

³J. Soures, L. M. Goldman, and M. Lubin, Nucl. Fu-

sion **13**, 829 (1973).

⁴B. L. Henke and M. A. Tester, *Advances in X-ray Analysis* (Plenum, New York, 1975), Vol. 18.

⁵S. Jackel, J. Albritton, E. B. Goldman, and S. Letzring, Bull. Am. Phys. Soc. **20**, 1335 (1975).

⁶E. G. McGuire, Phys. Rev. **185**, 1 (1968), and references therein.

⁷J. H. Scofield, Lawrence Livermore Laboratory Report No. UCRL-51326, 1973 (unpublished).

⁸G. Glupe and W. Mehlhorn, Phys. Lett. **25A**, 274 (1967); C. J. Powell, Rev. Mod. Phys. **48**, 33 (1976).

⁹G. Knop and W. Paul, in *Alpha, Beta, and Gamma Ray Spectroscopy*, edited by K. Siegbahn (North-Holland, Amsterdam, 1974), Chap. 1.

¹⁰L. N. Koppel, Lawrence Livermore Laboratory Report No. UCRL-75891, 1974 (unpublished); A. Hauer and G. Harvey, unpublished.

¹¹B. Yaakobi and A. Nee, Phys. Rev. Lett. **36**, 1077 (1976); B. Yaakobi and L. M. Goldman, to be published.

Tricritical Point in KH_2PO_4 †

V. Hugo Schmidt, Arthur B. Western, and Alan G. Baker

Department of Physics, Montana State University, Bozeman, Montana 59715

(Received 14 June 1976; revised manuscript received 21 July 1976)

A pressure-induced tricritical point is indicated for KH_2PO_4 near 2 kbar pressure. This estimate is based on analysis of our static dielectric data for pressures up to 3 kbar.

Tricritical points in an experimentally accessible three-dimensional space of the pressure, temperature, and electric field are possible in ferroelectrics. Peercy² found a tricritical point in SbSI near 235 K and 1.40 kbar. A proposal³ for a tricritical point in KH_2PO_4 (KDP) at high pressure was based on the fact that the critical field E_{cr} for KD_2PO_4 (DKDP) is 7100 V/cm,⁴ and only about 200 V/cm in KDP. The transition temperature T_c decreases from 223 K in DKDP to 123 K in KDP, and applying pressure to KDP reduces T_c until it approaches 0 K at 17 kbar,⁵ so one could expect that the tricritical pressure p_t required to reduce E_{cr} to zero would be much less than 17 kbar. A portion of the proposed phase diagram in pressure-temperature-electric-field space appears in Fig. 1.

To determine this phase diagram experimentally, we first measured E_{cr} at $p=0$ and obtained 232 ± 70 V/cm,⁶ in fair agreement with most of the other reported values. From electrocaloric experiments, Strukov *et al.*⁷ calculated $E_{\text{cr}} = 124$ V/cm. Reese⁸ found no latent heat for fields above 300 V/cm. From polarization measured as a function of temperature and bias field, Sid-

nenko and Gladkii⁹ found a critical field of 370 V/cm. From quasi-static tracing of hysteresis loops, Okada and Sugie¹⁰ obtained 160 V/cm for E_{cr} . Birefringence measurements of Vallade¹¹ lead to a critical field value of 254 V/cm. In contrast to these low values, Kobayashi, Uesu, and Enomoto¹² found $E_{\text{cr}} = 8500$ V/cm from x-ray dilatometric studies. Eberhard and Horn¹³ derived 6500 V/cm from thermal hysteresis of the ac dielectric susceptibility, but our reanalysis of their data taking other sources of hysteresis into account is consistent with a critical field near 300 V/cm.¹⁴

We report here our measurements of static dielectric behavior of a second KH_2PO_4 crystal at pressures of 0, 1, and 3 kbar; and using these results, we employ Landau theory¹⁵ to estimate the tricritical pressure p_t .

The $1 \times 1 \times 0.2$ cm³ crystal was prepared by Cleveland Crystals, Inc. with chrome-gold electrodes evaporated onto the large faces which are perpendicular to the ferroelectric c axis. No guard-ring configuration was used. The sample was suspended inside the pressure vessel which is enclosed by a double-walled cryostat immersed